ELSEVIER

Chemical Engineering Journal 133 (2007) 79–84

Chemical Engineering Journal

www.elsevier.com/locate/cej

# Dissolution kinetics of aluminum can in isopropyl alcohol for aluminum isopropoxide

Seung-Joon Yoo [a,*], Ho-Sung Yoon [b], Hee Dong Jang [b], Min-Jae Lee [a], Se-Il Lee [a], Seung Tae Hong [c], Hyung Sang Park [c]

[a] *Faculty of Environmental and Chemical Engineering, Seonam University, 720 Gwangchi-dong, Namwon 590-711, Republic of Korea*
[b] *Korea Institute of Geoscience and Mineral Resources, 30 Kajungdong, Yusongku, Daejeon 305-350, Republic of Korea*
[c] *Department of Chemical and Biomolecular Engineering, Sogang University, C.P.O. Box 1142, Seoul 100-611, Republic of Korea*

Received 26 July 2006; received in revised form 16 January 2007; accepted 2 February 2007

**Abstract**

A kinetic study of dissolution reaction of Al can waste was conducted for the synthesis of aluminum isopropoxide (AIP). With the used Al can and isopropyl alcohol (IPA) as reactants, the reaction was examined at the condition of 3 mol IPA/mol Al of stoichiometric ratio, adding $10^{-3}$ mol $HgI_2$/mol Al for catalyst and no agitation at the reaction temperature ranging from 70 to 82 °C. After 17 h, the reaction gave a 75% yield. A two-stage dissolution mechanism was proposed in which the dissolution rate is determined first by a chemical reaction and then by ash layer diffusion. On the basis of the shrinking core model with the shape of flat plate, the first dissolution rate of Al can was controlled by chemical reaction. The concentration of isopropyl alcohol was added to the reaction at the stoichiometric ratio, then it was largely changed through the dissolution reaction. Therefore, since the conversion rate of isopropyl alcohol varies greatly depending on the reaction time, it was included as an integral term of the reaction time. By using the Arrhenius expression, the apparent activation energy of the first chemical reaction step was determined to be 92.4 kJ $mol^{-1}$. In the second stage, the dissolution rate is controlled by diffusion control through the ash layer. The apparent activation energy of the second step was determined to be 174.9 kJ $mol^{-1}$.


*Keywords:* Kinetics; Dissolution; Aluminum can; Flat plate; Aluminum isopropoxide; Chemical reaction; Ash layer diffusion

## 1. Introduction

In the process of aluminum can recycling until now, the collected Al cans have been cut into pieces, washed, dried, melted in the furnace and finally reproduced as an aluminum ingot. In the conventional recycling process, the upper surface layer of the molten Al solution is oxidized to alumina by water and oxygen in air. This oxidized surface layer is called "aluminum dross". Commonly, the yield is diminished to 20–30% because of the formation of the aluminum dross in the process. However, this method of synthesizing aluminum alkoxide from Al can was able to completely eliminate the aluminum dross produced as a side product in the conventional Al can recycling process.

Depending on the type of bonded alcohol groups, aluminum alkoxide has various compounds such as aluminum ethoxide (AE, $Al(OC_2H_5)_3$) [1], aluminum isopropoxide (AIP, $Al(OC_3H_7)_3$) [2–4], aluminum sec-butoxide (ASB, $Al(OC_4H_9)_3$) [5,6]. Among these aluminum alkoxides, AIP has been used as a starting material for alumina product with high purity and high activation by sol–gel method, a catalyst in preparing the biodegradable polyester or in producing the ethyl acetate by the Tischenko reaction of acetaldehyde [7], but because of high price of alkoxide material, it has not been used widely in the industries, limited only to the laboratory use. To reduce the production cost of aluminum alkoxide, we synthesized aluminum alkoxide by using the used Al cans as a reactant.

The AIP is synthesized through dissolution reaction and vacuum distillation in the separation process, and the key reaction in the synthesis is the dissolution reaction of aluminum. To gain a clear understanding of the dissolution reaction of aluminum cans, we examined the reaction kinetics of the used aluminum cans. For the synthesis of AIP of high purity from the used Al cans, it is necessary to optimize process variables and conditions such as reaction time, temperature, concentration of reactants.

* Corresponding author. Tel.: +82 63 620 0230; fax: +82 63 620 0211.
*E-mail address:* sjyoo001@hanmail.net (S.-J. Yoo).

1385-8947/$ – see front matter © 2007 Elsevier B.V. All rights reserved.
doi:10.1016/j.cej.2007.02.003

**Nomenclature**

| | |
|---|---|
| AIP | aluminum isopropoxide |
| $C_A$ | concentration of Al reactant (mol $L^{-1}$) |
| $C_{A0}$ | initial concentration of Al reactant (mol $L^{-1}$) |
| $C_B$ | concentration of IPA reactant (mol $L^{-1}$) |
| $C_{B0}$ | initial concentration of IPA reactant (mol $L^{-1}$) |
| $D_e$ | effective diffusion coefficient |
| $E_A$ | apparent reaction rate constant for ash layer diffusion ($s^{-1}$) |
| $E_C$ | apparent activation energy for chemical reaction (kJ $mol^{-1}$) |
| IPA | isopropyl alcohol |
| $k$ | first-order rate constant for the surface reaction (m $s^{-1}$) |
| $k_A$ | apparent rate constant for ash layer diffusion ($ms^{-1}$) |
| $k_c$ | apparent rate constant for chemical reaction (m $s^{-1}$) |
| $N_A$ | moles of Al reactant (mol) |
| $N_B$ | moles of IPA reactant (mol) |
| $N_{B0}$ | initial moles of IPA reactant |
| $l$ | thickness of unreacted layer in Al can (m) |
| $L$ | initial thickness of Al can (m) |
| $Q_B$ | flux of IPA within the ash layer |
| $S_{ex}$ | external surface area ($m^2$) |
| $t$ | time (s) |
| $T$ | temperature (K) |
| $X_A$ | fraction of converted Al |
| $X_B$ | fraction of converted IPA |

*Greek letter*

| | |
|---|---|
| $\rho_A$ | molar density of Al component included in Al can (mol $L^{-1}$) |

The AIP compound was synthesized using Al can scraps and IPA as reactants on the basis of the following stoichiometric Eq. (1):

$$Al_{can}(s) + 3C_3H_7OH(l) \rightarrow Al(OC_3H_7)_3 + \frac{3}{2}H_2 \uparrow + \text{residue} \quad (1)$$

Fig. 1 shows the schematic diagram of dissolution reaction between Al can and IPA.

### 1.1. Chemical reaction control

Assuming the first order chemical reaction rate model based on shrinking core model [8,9] that has the shape of flat plate. The chemical reaction may be expressed in the following Eq. (2):

$$-\frac{1}{S_{ex}}\frac{dN_A}{dt} = -\frac{\rho_A}{S_{ex}}S_{ex}\frac{dl}{dt} = -\rho_A\frac{dl}{dt} = \frac{1}{3}kC_B \quad (2)$$

However, the variation of $C_B$ is too big to be neglected during the chemical reaction.

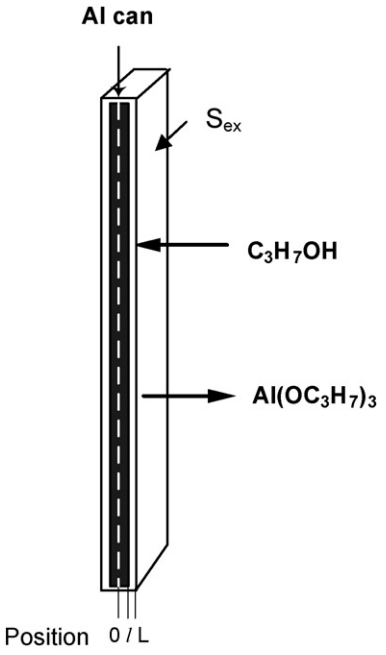


Fig. 1. Representation of a reacting Al can.

Since $C_B$ cannot be accepted constant in Eq. (2), this model is modified as follows:

$$-\rho_A\int_L^l dl = \frac{1}{3}k_s\int_0^t dt \quad (3)$$

$$\frac{3\rho_A L}{k}\left(1-\frac{l}{L}\right) = \int_0^t C_{B0}(1-X_B)\,dt \quad (4)$$

$$X_A = k_C\int_0^t (1-X_B)\,dt \quad (5)$$

where $k_C$ is the apparent rate constant for chemical reaction.

$$k_c = \frac{C_{B0}k}{3\rho_A L} \quad (6)$$

### 1.2. Ash layer diffusion control

During the chemical reaction, Al component in the Al can is dissolved into the solution. The ash layer of the chemically reacted Al can become increasingly thicker. Therefore, the diffusion through the ash layer acts as the reaction rate control step in the second stage. At this time, the boundary line ($l$) of the unreacted layer in Al can moves into the center. The reaction rate can be expressed in terms of the diffusion rate of IPA through the ash layer of the Al can.

$$-\frac{1}{S_{ex}}\frac{dN_A}{dt} = Q_B \quad (7)$$

$$-\frac{dN_A}{dt} = S_{ex}D_e\frac{dC_B}{dl} \quad (8)$$

If it is integrated at interval from $L$ to $l$ and then at interval from 0 to $t$ time, the rate equation may be modified as follows:

$$\int_0^t C_B \, dt = \frac{\rho_A L^2}{D_e}\left(1 - \frac{l}{L}\right)^2 \quad (9)$$

$$X_A^2 = k_A \int_0^t (1 - X_B)\, dt \quad (10)$$

where $k_A$ is the apparent rate constant for ash layer diffusion:

$$k_A = \frac{C_{B0} D_e}{3\rho_A L^2} \quad (11)$$

## 2. Materials and methods

The used Al cans were cut into small scraps on a shredder and then heat-treated for 1 h at the calcination condition of 600 °C to remove the lacquer, pigment, coated plastics and other polluted materials.

Firstly, the reaction temperature in the reactor with isopropyl alcohol (IPA, $C_3H_7OH$, >99%, Daejung Chemicals) of 3 mol/mol Al as a reactant and $10^{-3}$ mol $HgI_2$/mol Al for catalyst ($HgI_2$, mercuric iodide, >99%, Fluka) was controlled by Pyrex double jacket reactor circulating water, and then Al can scraps were added to the reactor. The role of the catalyst has not been understood completely until now, but it is known that the surface oxide layers on the Al can was softened and amalgamated by catalyst [10–12]. At this time, the effect of reaction temperature was observed at 70, 75, and 82 °C because the AIP generated becomes solidified at a reaction temperature lower than 70 °C. Since the Al can scraps bigger than 1 cm were stuck on the reactants at the agitation by the impeller, the reaction was performed at the condition of no mixing.

The Al concentration was analyzed by measuring the weight of the Al cans according to the dissolution reaction times. The IPA concentration was analyzed on a Gas Chromatographer (HP 5890, Hewlett-Packard 5890 Series II).

## 3. Results and discussion

Fig. 2 presents the Al conversion rate during the dissolution reaction. The rate of Al conversion could be divided into two reaction stages on the basis of reaction time of 50 min: a rapid reaction stage and a slow reaction stage.

Fig. 3 shows the result of analyzing the SEM photographs of Al can surface at the dissolution temperature of 82 °C. As shown in Fig. 3(a), the surface of the initial Al can, shows a little rough state than original Al can due to evaporation of volatile components existed in and on the Al can during the pretreatment. On the other hand, Fig. 3(b) shows that the reacted Al surface after 50 min was very rough with chemical reaction, revealing some of the Al components remained on the surface of Al can. Fig. 3(c) shows that only the ash layer remained after the complete dissolution reaction.

Fig. 4 shows the changes in reaction temperature in the reactor by exothermic reaction during the dissolution reaction. The temperature of dissolution reaction increased rapidly for 50 min after the start, and then decreased slowly to equilibrium temperature. However, at 82 °C, the reaction temperature did not show any changes during the entire dissolution reaction because the boiling point of IPA is 82 °C, the latent heat of IPA offset the increase in dissolution reaction heat.

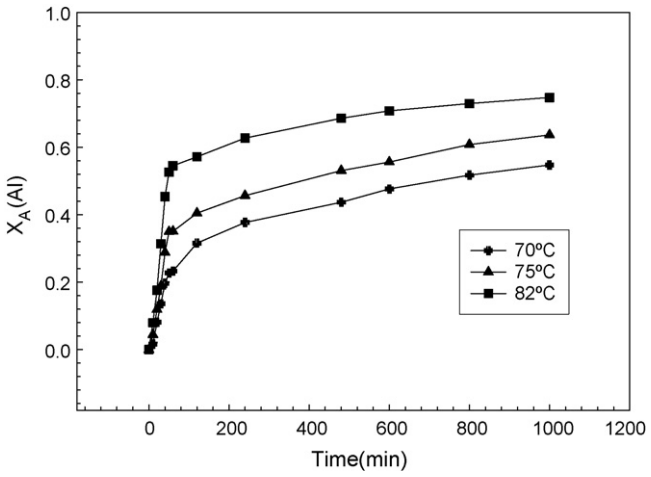


Fig. 2. Evolution of Al conversion ($X_A$).

On the basis of the results described above, the dissolution reaction time of 50 min was set as a criterion for determining the two stage reaction intervals.

In this experiment, the concentration of IPA was added at the stoichiometric ratio of 3 mol/mol Al on the basis of Al component in the Al can scraps, and it was greatly decreased during the dissolution reaction. The concentration of IPA with respect to the reaction times was analyzed as shown in Fig. 5.

$X_B$ equation shown in Table 1 is the result obtained by regression of the experimental $X_B$ data where the experimental data of $X_B$, was fitted by the basic equation of $X_B = y_0 + (at/(b+t))$ and then the estimated parameters of $y_0$, $a$, $b$ were determined through regression.

When these parameters obtained in Table 1 are replaced in $\int_0^t (1 + X_B)\, dt$, the final equations in Table 2 were obtained.

Table 1
Parameter values of IPA conversion by $X_B = y_0 + (at/(b+t))$ according to dissolution temperature

| Parameter | Reaction temperature (°C) | | |
|---|---|---|---|
| | 70 | 75 | 82 |
| $y_0$ | −0.05882 | −0.08322 | −0.1043 |
| $a$ | 0.7432 | 1.023 | 1.1503 |
| $b$ | 159.5 | 129.7 | 41.9187 |

Table 2
Equations of $\int_0^t (1 + X_B)\, dt$ according to dissolution temperature

| Temperature (°C) | $\int_0^t (1 + X_B)\, dt$ |
|---|---|
| 70 | $0.3157t + 118.539 \ln \lvert 214.61 + 1.3455t \rvert - 118.539$ |
| 75 | $0.06022t + 132.683 \ln \lvert 126.78 + 0.9775t \rvert - 132.683$ |
| 82 | $-0.046t + 48.219 \ln \lvert 36.44 + 0.8693t \rvert - 48.219$ |

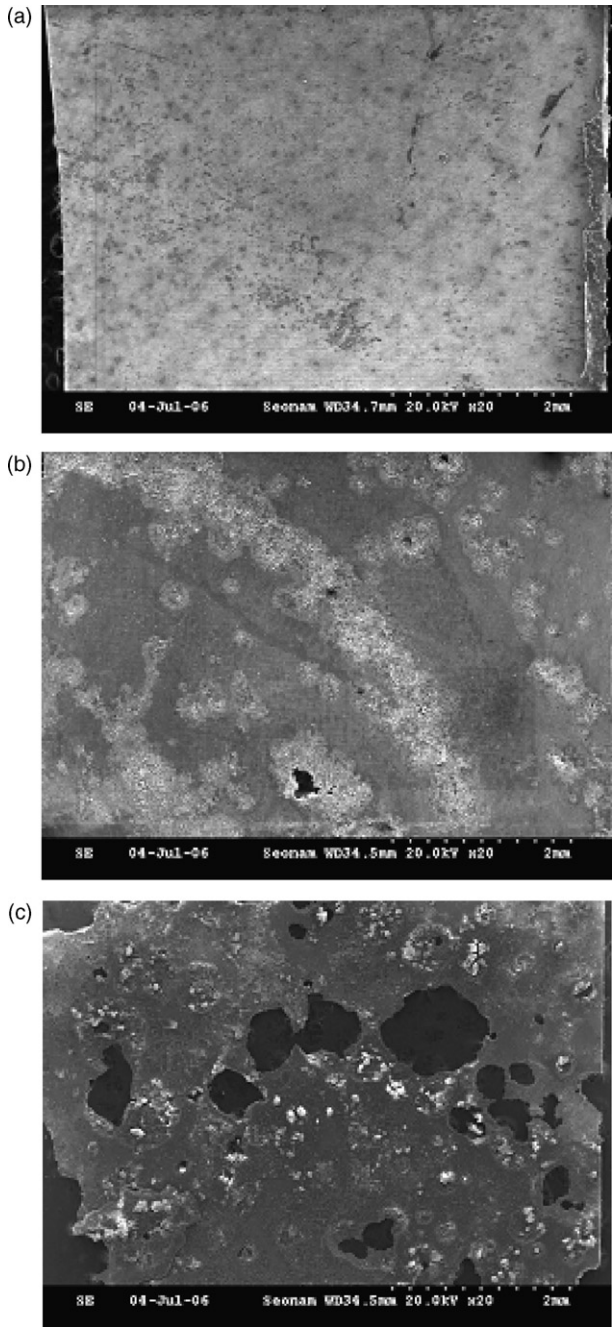


Fig. 3. SEM photographs of Al can surface according to dissolution reaction times: (a) 0 min; (b) 50 min; (c) 1000 min.

### 3.1. Chemical reaction control

In the initial chemical reaction stage, the reaction rate changed rapidly, and we observed that the reaction rate depended largely on the reaction temperature in this experiment. The chemical reaction took about 50 min.

The rate equation can be summarized as in Eq. (5) using the shrinking core model that has the shape of planar plate. On the basis of model equation (5), the apparent rate constant ($k_c$) can be calculated by the least square method according to reaction temperatures as shown in Fig. 6.

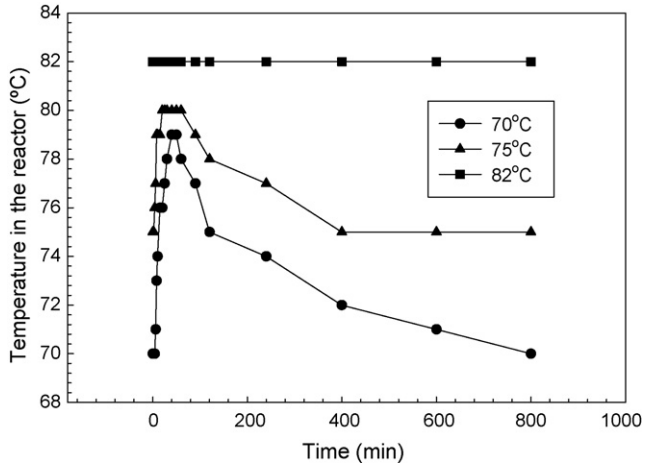


Fig. 4. Variation of temperature in the reactor.

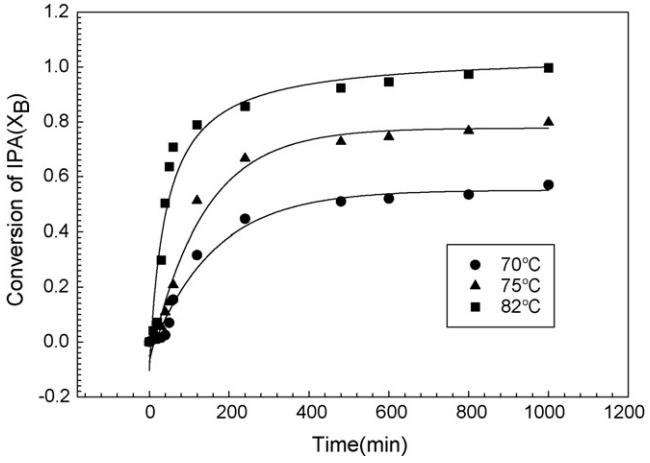


Fig. 5. Evolution of IPA conversion ($X_B$).

To examine the effect of the reaction temperature, the apparent activation energy was calculated by rate constants according to the temperatures. In the case of the chemical reaction control, the apparent activation energy was calculated at 92.4 kJ mol$^{-1}$ in the range of 70–82 °C in this experiment as shown by Fig. 7.

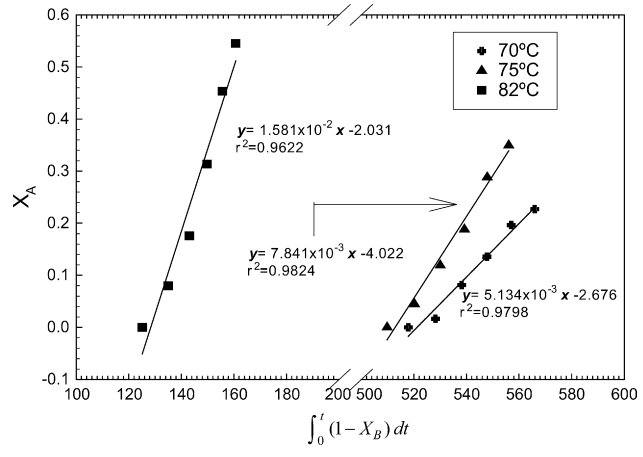


Fig. 6. The variation in $X_A$ vs. $\int_0^t (1 - X_B)\,dt$.

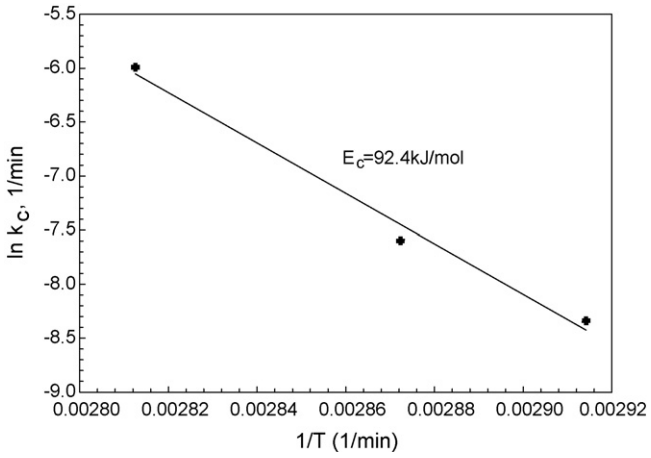


Fig. 7. Arrhenius plot for chemical reaction control stage.

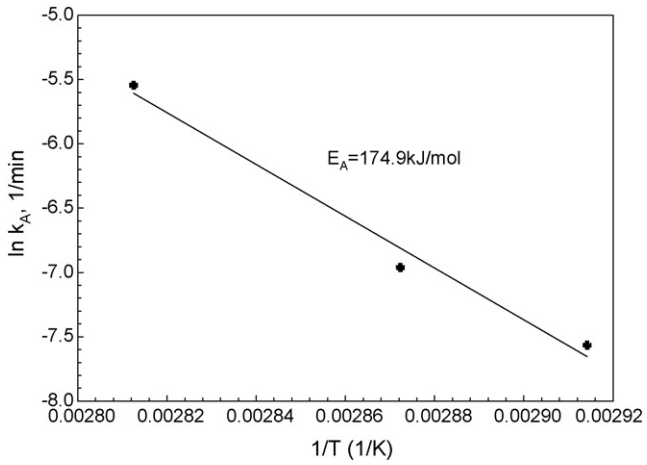


Fig. 9. Arrhenius plot for ash layer diffusion control step.

### 3.2. Ash layer diffusion control

In the case of the ash layer diffusion control, the rate equation can be summarized by following Eq. (10) by shrinking core model. The reaction rate increased slowly by the ash layer diffusion from the 50 min point to 1000 min which is the end of reaction. On the basis of model equation (10), Fig. 8 shows the apparent rate constant ($k_A$) calculated by the least square method according to the reaction temperatures.

To examine the dependence of reaction temperature, the apparent activation energy was calculated by using the Arrhenius expression from the rate constant as shown in Fig. 9. The activation energy was 174.9 kJ mol$^{-1}$ as shown in Fig. 9.

In general, temperature dependence is high in the stage of chemical reaction control but low in the stage of ash layer diffusion [13,14]. In this experiment, however, the apparent activation energy in the ash layer diffusion stage was higher than that in the chemical reaction stage. It seems to be affected by mixing. As the reaction temperature increased to the IPA boiling point, the solution came to a boil and the temperature dependence became greater because of the mixing effect caused by the boiling of solution.

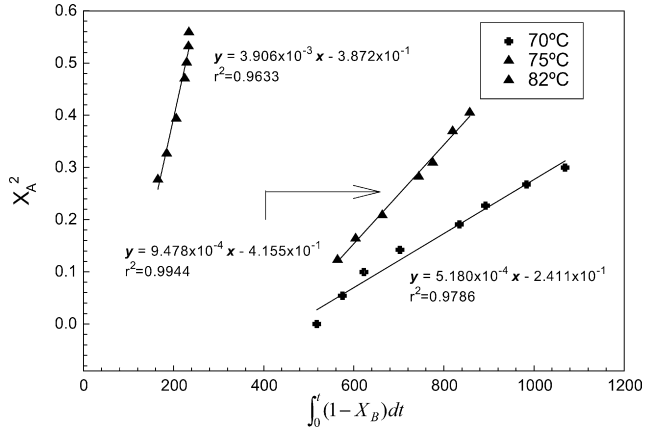


Fig. 8. The variation in $X_A^2$ vs. $\int_0^t (1 - X_B)\,dt$.

In this experiment, the reactor was maintained with no agitation during the reaction because the reaction finally stopped when the impeller was stuck with the reactants greater than 1 cm in size. Therefore, temperature dependence appeared even higher because the increase in the reaction temperature to the boiling point of IPA brought an increase in the diffusion rate in the reactor even without mixing.

## 4. Conclusions

In this paper, we proposed a two stage model in the dissolution reaction of used Al can, the chemical reaction, and ash layer diffusion.

(1) In the initial chemical reaction control stage, the dissolution kinetics follows a shrinking core model with chemical reaction as the first rate-controlling step. Especially, an increase in the reaction temperature accelerates the chemical reaction rate considerably. The apparent activation energy was determined to be 92.4 kJ mol$^{-1}$ at the range of 70–82 °C. The postulated reaction was conformed by both the value of the apparent activation energy and the linear relationship of the rate constant and activation energy.
(2) In the second ash layer diffusion stage, the apparent activation energy was determined to be larger value (174.9 kJ mol$^{-1}$) than the activation energy of the chemical reaction control stage. Temperature dependence in the ash layer diffusion step was enhanced larger than the chemical reaction control stage in the range of 70–82 °C because the increase in the reaction temperature must have led to an increase in the diffusion rate.

In conclusion, the dissolution reaction rate was very sensitive to the temperature in the range of 70–82 °C. The two stage reaction mechanism proposed in this study agrees with the experimental results and well explains the dissolution reaction of the used Al can, the chemical reaction, and the ash layer diffusion.

## Acknowledgement

The research was supported by the Korea Institute of Geoscience and Mineral Resources of South Korea.

## References

[1] R.C. Wilhoit, J.R. Burton, F.-T. Kuo, S.-R. Huang, A. Viquesnel, Properties of aluminum ethoxide, J. Inorg. Nucl. Chem. 24 (1962) 851–861.
[2] N.Y. Turova, V.A. Kozunov, A.I. Yanovskii, N.G. Bokii, Y.T. Struchkov, B.L. Tarnopol'skii, Physico-chemical and structural investigation of aluminum isopropoxide, J. Inorg. Nucl. Chem. 41 (1979) 5–11.
[3] K. Folting, W.E. Streib, K.G. Caulton, O. Poncelet, L.G. Hubert-Pfalzgraf, Characterization of aluminum isopropoxide and aluminosiloxanes, Polyhedron 10 (1991) 1639–1646.
[4] A. Abraham, R. Prins, J.A. van Bokhoven, E.R.H. van Eck, A.P.M. Kentgens, Multinuclear solid-state high-resolution and $^{13}$C-{$^{27}$Al} double-resonance magic-angle spinning NMR studies on aluminum alkoxides, J. Phys. Chem. B 110 (2006) 6553–6560.
[5] F. Babonneau, L. Coury, J. Livage, Aluminum sec-butoxide modified with ethylacetoacetate: an attractive precursor for the sol–gel synthesis of ceramics, J. Non-Cryst. Solids 121 (1990) 153–157.
[6] R.J.M.J. Vogels, J.T. Kloprogge, P.A. Buining, D. Seykens, J.B.H. Jansen, H.W. Geus, The tridecameric aluminum complex as an appropriate precursor for fibrous boehmite: a $^{27}$Al NMR study on the partial hydrolysis of aluminum sec-butoxide, J. Non-Cryst. Solids 191 (1995) 38–44.
[7] Y. Ogata, A. Kawasaki, I. Kishi, Kinetics of the Tischenko reaction of acetaldehyde with aluminum isopropoxide, Tetrahedron 23 (1967) 825–830.
[8] O. Levenspiel, Chemical Reaction Engineering, 3rd ed., John Wiley & Sons Inc., New York, 1999.
[9] L.D. Schmidt, The Engineering of Chemical Reactions, 2nd ed., Oxford University Press, 2005.
[10] S.-J. Yoo, H.-S. Yoon, H.D. Jang, J.-W. Lee, S.-T. Hong, M.-J. Lee, S.-I. Lee, K.-W. Jun, Synthesis of aluminum isopropoxide from aluminum dross, Korean J. Chem. Eng. 23 (2006) 683–687.
[11] S.-J. Yoo, Process for preparation of aluminum alkoxide from aluminum waste, Korean Patent No. 509395 (2005).
[12] W.W. Webar, T.J. Weeks Jr., Process and apparatus for preparing aluminum alkoxides, European Patent No. 0018037B1 (1980).
[13] F. Bakan, O. Lacin, B. Bayrak, H. Sarac, Dissolution kinetics of natural magnesite in lactic acid solutions, Int. J. Miner. Process. 80 (2006) 27–34.
[14] B. Bayrak, O. Lacin, F. Bakan, H. Sarac, Investigation of dissolution kinetics of natural magnesite in gluconic acid solutions, Chem. Eng. J. 117 (2006) 109–115.